Characterization of Thermal and Frequency-Dispersion Effects in GaAs MESFET Devices

J. Rodriguez-Tellez, T. Fernandez, A. Mediavilla, and A. Tazon

***Abstract*—New simple and accurate measurement procedures that enable the dispersion and thermal effects in GaAs MESFETs to be observed independently are presented in this paper. The results indicate that the differences observed between the static and pulsed characteristics of the device are not solely due to thermal effects, as is sometimes thought. Electrical and thermal measurements also show the GaAs MESFET to take a relatively long time before the effect of self-heating manifests itself on the IV characteristics of the device.**

***Index Terms*—Dynamic IV characteristics, frequency dispersion, GaAs MESFET, thermal effects.**

I. Introduction

Over recent years, a number of papers have clearly demonstrated the effect of heating, the effect of frequency dispersion, and the strong dependency of the latter on the former in the electrical characteristics of GaAs MESFETs [1]–[3]. Although these measurement schemes enable these effects to be observed, a measurement system that enables the effects of dispersion and the effects of temperature to be investigated independently in an easy and accurate manner is not available.

In this paper, a measurement system is described that enables the frequency-dispersion effect to be measured independently of temperature effects. The same system can also be used to measure and control the heating arising from the biasing to the device.

II. Measurements

The measurement system developed to investigate the frequency-disperison and thermal effects in GaAs devices includes two pulse generators and two dc supplies, which, for testing a MESFET, are configured as shown in Fig. 1 [4]. The software enables the following measurements to be performed.

1) *dc IV measurements*. These can be performed over a 0–30-V range and, since the design is capable of delivering a current of 2 A, a wide range of devices can be measured. A user-specified delay time enables the time (after the bias voltages are applied) before the drain current is measured to be defined. This is useful in assessing the self-heating effect from a dc point-of-view.
2) *Pulsed IV measurements*. These can also be performed over a 0– 30-V range with current levels of up to 2 A. These dynamic measurements can be performed in a variety of ways such as: 1) pulsing the gate–source terminal while the drain–source terminal is swept in a normal dc fashion; 2) pulsing the drain–source terminal while the gate–source terminal is swept in a normal dc fashion; and 3) pulsing the drain–source and gate–source terminals together. From the point-of-view of ensuring that the self-heating effect is minimized it is, of course, not necessary to pulse both terminals. Pulsing either is sufficient, providing the drain–source resistance of the device is high when it is switched off. The amplitude of the pulses and the static voltages from the dc supplies are user defined. This enables the static and dynamic conditions used for the measurements to be controlled and the effect of the self-heating on the dispersion effect to be observed. To cater for devices with fast thermal response times, pulsewidths as short as 10 ns with pulse periods of 0.1 s can be employed in this system.
3) *Ambient temperature measurements*. The measurements described above, if repeated as a function of ambient temperature, enable the effects of temperature and the effects of frequency dispersion to be observed in an easy and straightforward manner. The temperature range can extend from −80 °C to 150 °C.

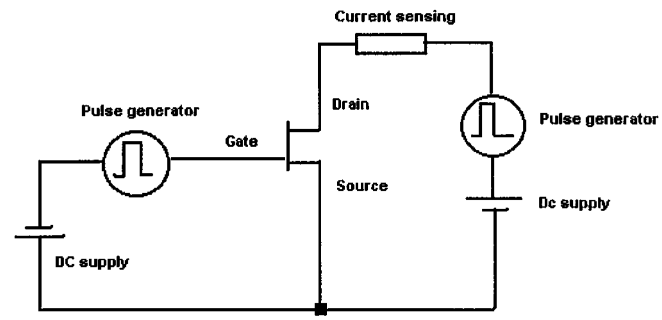

Fig. 1. Two-pulse measurement system.

III. Devices Considered

The tests described were implemented on a sample consisting of several hundred 0.5-μm gatelength −0.8-V pinchoff MESFETs of varying gatewidths. These devices were from the same wafer and were produced using an ion-implanted process on a liquid encapsulated czochralski (LEC) substrate. Ti/Pt/Au gate metallization with silicon–nitride passivation was used.

Since it is not possible to show the results for all the devices considered, a four-finger 225-μm gatewidth per finger (900-μm gatewidth in total) MESFET will be used as the main demonstrator. Similar trends in the measured data were observed with the other devices considered. Extensive thermal data for these devices can be found in [5].

IV. Variable Delay-Time DC Results

The issue of self-heating was initially considered by measuring the dc output characteristics of the device with different delay times. The results of this at one specific bias point are shown in Fig. 2. This shows the drain current at $V_{\rm GS} = 0$ V, $V_{\rm DS} = 4$ V as a function of delay time. The bias point selected falls well in the saturation region where the self-heating effect should be highly significant. The temperature of the device is also shown in this figure and was measured with the use of liquid crystals [5], [6].

As can be seen, no significant change to the drain current occurs until the delay time reaches 10 ms and, even after a 1-s delay, the drop in the drain current is only 1 mA. Although others [7], [8] have also shown the device to take a relatively long time before the self-heating effect manifests itself on the IV characteristics, this issue will be reexamined later using a different measurement approach. The results confirm that, even with a 1-s delay, the temperature of the device is not unduly high. The 50 °C base temperature shown in this figure arises from the heating caused by the previous $V_{\rm DS}$ points included in the measurements. It should be remembered that Fig. 2 corresponds to only one bias point in the output characteristics measured. The thermal impedance of this device was measured to be 122 °C/W at $V{\rm gs} = 0$ V, $V{\rm ds} = 3$ V.

Manuscript received November 12, 1999; revised December 15, 2000.

J. Rodriguez-Tellez is with the Electrical Engineering Department, University of Bradford, Bradford BD7 1DP, U.K.

T. Fernandez, A. Mediavilla, and A. Tazon are with the Department of Communications Engineering, University of Cantabria, Santander 39005, Spain.

Publisher Item Identifier S 0018-9480(01)05058-X.

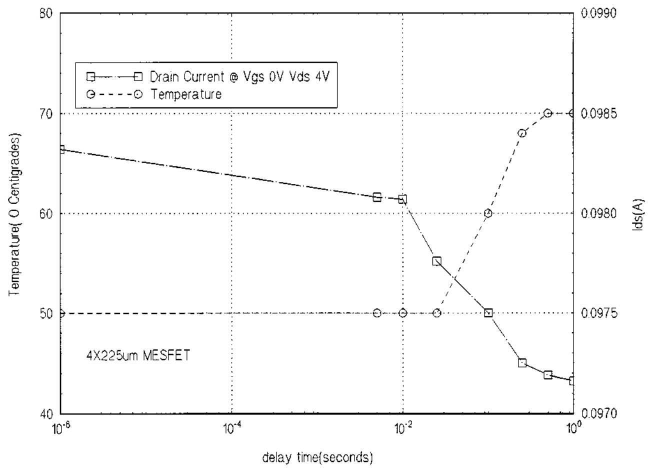

Fig. 2. DC drain current and temperature versus delay time.

V. Variable Pulsewidth/Period Results

In order to check the self-heating results presented earlier, the dynamic output characteristics of the device were measured using a variety of pulsewidth conditions with the static supplies set to $V_{\mathrm{GS}} = -1$ V, $V_{\mathrm{DS}} = 0$ V. For this test, the gate–source and drain–source junction were pulsed. A pulse period of 0.1 s (corresponding to a measurement frequency of 10 Hz) was employed. This measurement frequency is low enough to ensure that the frequency-dispersion effect is minimal. The dynamic point corresponding to $v_{\mathrm{gs}} = 0$ V, $v_{\mathrm{ds}} = 4$ V was measured to check the results presented earlier. Although the test commenced with very narrow (10 ns) pulsewidths, it was not until the pulsewidth reached 10 ms that a change in the drain current (0.2 mA) was noticed. This agrees quite well with the results from the variable delay time dc measurements and with the observations made by others on this issue [7], [8].

In view of the above results, a pulsewidth in the microsecond range should ensure that any possible self-heating arising from the dynamic bias conditions does not alter the electrical characteristics of the device. However, for some fast high electron-mobility transistor (HEMT) or heterojunction bipolar transistor (HBT) devices, pulsewidths smaller than this may be needed.

To determine the upper frequency point at which the frequency-disperison effect settles, dynamic pulse measurements using 1-μs-wide (300-ns rise and fall times) pulses with varying periods were performed. For these tests, the static conditions employed were $V_{\mathrm{GS}} = -1$ V, $V_{\mathrm{DS}} = 0$ V and the dynamic characteristics over a wide operating area (v_{gs} from -1 to 0 V and v_{ds} from 0 to 4 V) were measured. This test revealed that when a measurement frequency in the 40–200-Hz range was employed (pulse period of 5–25 ms), the dynamic characteristics of the device varied rapidly. This change in the characteristics with increasing frequency lessened considerably beyond 200 Hz and after 800 Hz became reasonably settled. A measurement frequency of 1 kHz, therefore, seems appropriate for the purposes of comparing the dynamic characteristics after the frequency-disperison effect has taken place, with the very low-frequency or dc characteristics.

VI. Pulsed Results

Fig. 3 shows a number of curves measured under static and pulsed conditions using pulsewidths of 1 μs with a pulse period of 1 ms (corresponding to 1-kHz measurement frequency). The curve for the static case corresponds to $V_{\mathrm{GS}} = 0$ V, and was measured with a 1-s delay time between points to ensure that the self-heating effect reaches equilibrium conditions. The remaining curves were measured under different pulsed conditions. For all these pulsed cases, the end or dynamic value of v_{GS} corresponds to 0 V so that the pulsed curves can be compared with the static curve.

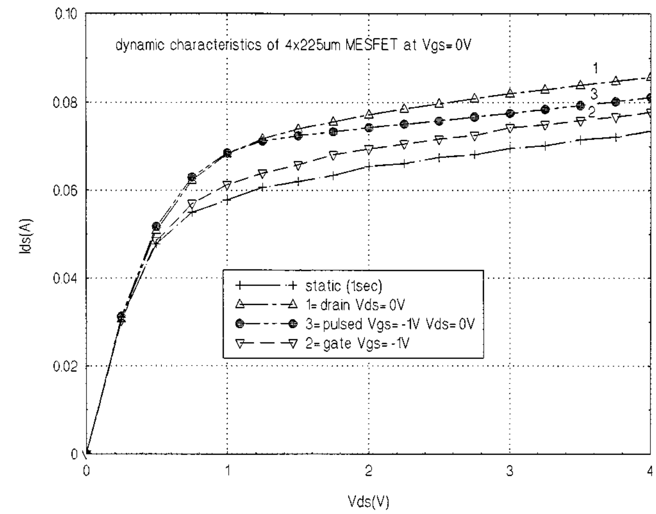

Fig. 3. Pulsed IV characteristics of 900-μm MESFET at $V\mathrm{gs} = 0$ V.

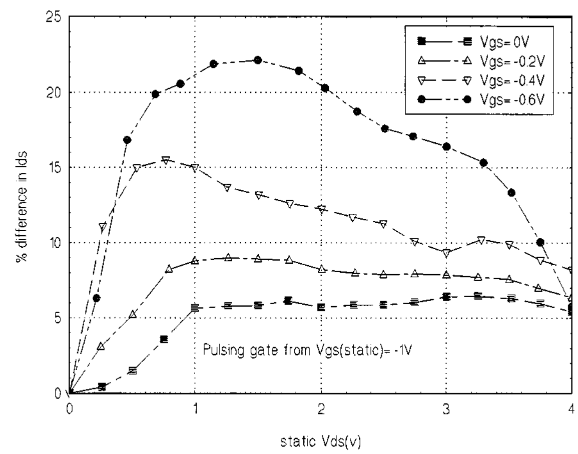

Fig. 4. Percentage difference in drain–source current when gate is pulsed.

Curve 1 corresponds to the case where the drain–source terminal is pulsed from the static point of $V_{\mathrm{DS}} = 0$ V with the gate–source terminal fixed at $V_{\mathrm{GS}} = 0$ V. Since the measurement frequency is 1 kHz, this curve represents the IV behavior of the device after the frequency-disperison effect has taken place. The difference between curve 1 and the static curve is, therefore, due to frequency-disperison and temperature effects. For the static curve, the drain–source resistance of the device is 230 Ω and this reduces to 192 Ω when the device drain terminal is pulsed.

Curve 2 corresponds to the case where the gate–source terminal is pulsed from the static point of $V_{\mathrm{GS}} = -1$ V, where the device is firmly pinched off, and the drain–source terminal is swept in a normal dc manner. Since the self-heating effect and ambient temperature of the device will be the same for curves 1 and 2, it follows that the difference between these two curves is due to frequency-disperison effects. The difference between curve 2 and the static curve is due to frequency-disperison and temperature effects. For curve 2, the drain–source resistance is 216 Ω, which is closer to the dc value than when the drain terminal is pulsed.

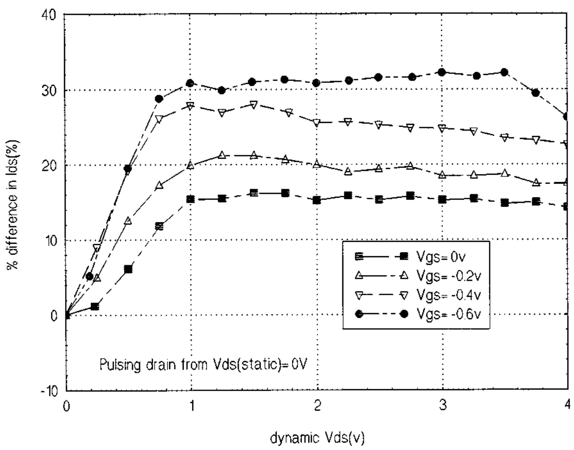

Fig. 5. Percentage difference in drain current when drain is pulsed.

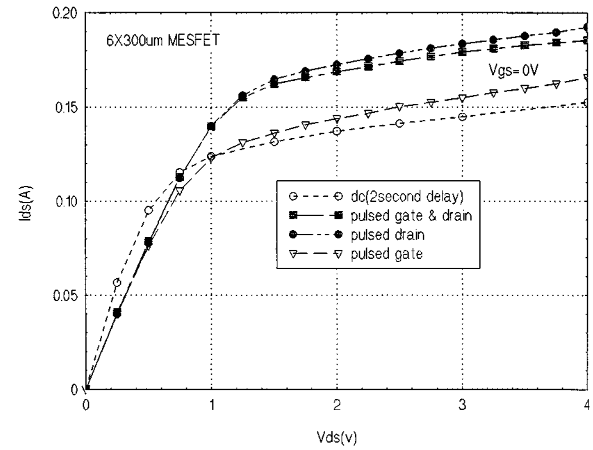

Fig. 6. Pulsed IV characteristics of 1800-μm MESFET at $V\text{gs} = 0$ V.

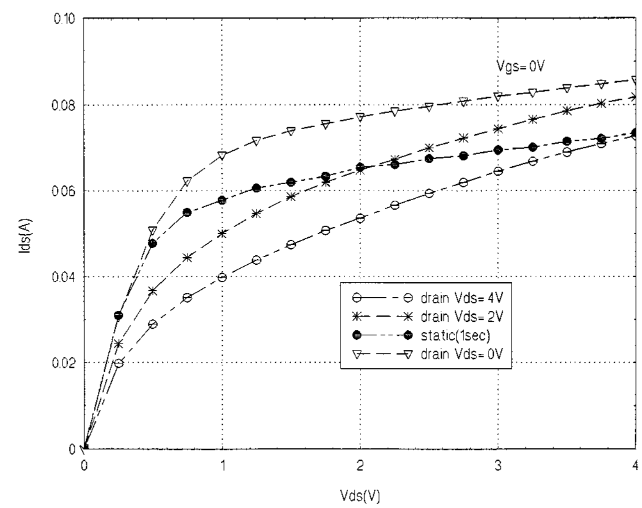

Fig. 7. Pulsed IV curves under different static bias conditions.

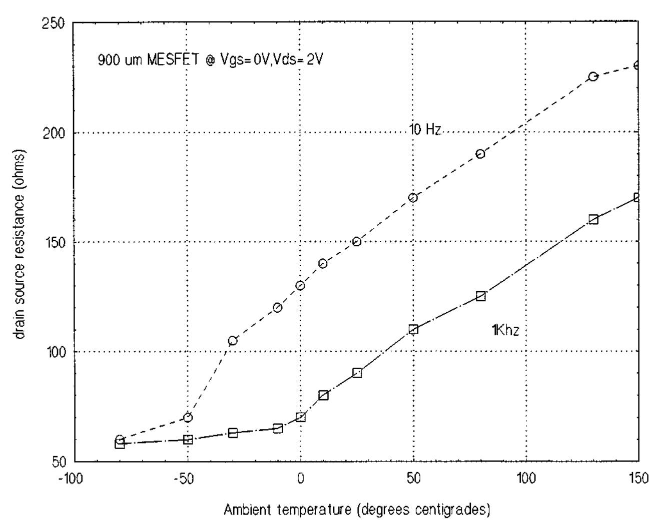

Fig. 8. Drain–source resistance versus ambient temperature for 900-μm device.

The final interesting case to consider is curve 3, which corresponds to the situation where both the gate– and drain–source terminals are pulsed. For this situation, the gate is pulsed from the static point of $V_{\text{GS}} = -1$ V and the drain pulsed from the static point of $V_{\text{DS}} = 0$ V. From a thermal point-of-view, this situation is the same as curves 1 and 2. The results, however, differ considerably from the two earlier pulsed cases. These pulsed results illustrate the dependence of the dispersion effect on the electric-field conditions, which are different for the three cases considered. The change in the electric-field conditions varies the trap occupancy due to the change in the Fermi level. The pulsed IV characteristics shown are, therefore, specific to the conditions (bias and temperature) employed.

Although the dispersion effect is often highlighted under high current conditions in the saturation region (as in Fig. 3), this should be treated with caution. If the dispersion effect is dependent on the electric-field conditions, then this should also be evident in the linear region. This is demonstrated in Figs. 4 and 5, which show the percentage difference between the static and pulsed drain current as a function of v_{ds} and v_{gs}. Here, we can see an almost linear dependency of the dispersion effect on the electric field when the voltage on the gate– or drain–source is varied in the linear region. This dependency reaches a steady value when the channel is saturated. Notice also that pulsing the gate or drain produces a similar percentage difference for the same unit change in electric field in the linear region.

To illustrate that the general trend of the data is true for the other devices considered, in Fig. 6, we show the corresponding information for an 1800-μm gatewidth (six fingers of 300-μm/finger gatewidth) device from the same wafer. As can be seen, the general behavior of the data is the same as for the previous device. The thermal impedance of this device was measured to be 123 °C/W at $V\text{gs} = 0$ V, $V\text{ds} = 3$ V.

The pulsed measurements can, of course, be carried out from any static bias position (and, if required, under isothermal conditions [7], [8]) and, by doing so, the self-heating effect can be defined. Fig. 7, for example, shows the behavior of the device when the drain–source terminal is pulsed from various V_{DS} static starting points with the gate–source fixed at 0 V. The $V_{\text{GS}} = 0$ V dc static curve (with 1-s delay) is superimposed on this figure for comparison purposes. The information shown in Fig. 7, while demonstrating that by altering the static bias significant self-heating can be introduced, should be viewed with caution. The possible assumption that the differences between Figs. 7 and 3 are due to the self-heating effect alone would be incorrect. Clearly, by adjusting the static bias, the self-heating has been altered, but by doing so, the dispersion effect has also been modified. This occurs not just because the temperature has altered, but also because the bias conditions (static and dynamic) employed in these two tests are different from those employed in Fig. 3. While the thermal effects could be removed from the characteristics shown in Fig. 7, an approach that provides additional insight is to perform the dynamic measurements from a static point where the device is

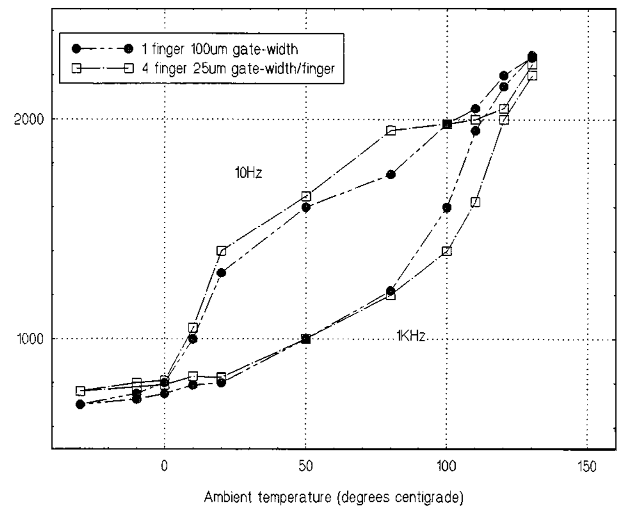

Fig. 9. Drain–source resistance for 100-μm devices composed of 1–4 fingers.

off (as in Fig. 3) as a function of ambient temperature. This enables the dependency of the dispersion effect on ambient temperature to be determined over a wide temperature range without the complications introduced by the static bias. The results of this are summarized in Fig. 8, which shows the drain–source resistance before (at 10 Hz) and after (at 1 kHz) the frequency-disperison effect. This data was measured from the static point of $V_{\rm GS} = 0$ V, $V_{\rm DS} = 0$ V by pulsing the drain terminal only and corresponds to the $v_{\rm gs} = 0$ V, $v_{\rm ds} = 2$ V dynamic point. The corresponding information for smaller devices is shown in Fig. 9 to illustrate the fact that under high- and low-temperature conditions, the device becomes free of the dispersion effect. This occurs because of the change in the Fermi level as the temperature is varied. This facilitates the release of electrons from the traps under high-temperature conditions and exhibits the process as the temperature and the Fermi level is lowered. The information in Fig. 9 clearly shows the significant effect that the number of fingers has on the thermal and dispersion characteristics of the device. The thermal impedance for the one-finger device was measured as 270 °C/W, whereas for the four-finger device, the value is 333 °C/W.

VII. Conclusions

A measurement system for quantifying the dependency of the frequency-disperison effect on electric field and temperature has been presented. This uses a pulsed IV measurement system and a thermally controlled wafer prober. The pulsed measurements can be performed by pulsing either the gate or drain or both terminals. The results presented indicate that the differences observed between the static and dynamic characteristics are to a significant extent due to frequency-disperison effects.

Pulsed IV measurements carried out in conjunction with liquid crystals show that a relatively long pulsewidth (approximately 10 ms) is required before the self-heating effect has a measurable effect on the IV characteristics of a medium-size power transistor.

References

[1] J. Rodriguez-Tellez, B. P. Stothard, and M. Al-Daas, "Static, pulsed and frequency-dependent IV characteristics of GaAs FETs," *Proc. Inst. Elect. Eng.*, pt. G, vol. 143, pp. 129–133, June 1996.

[2] ——, "Frequency and temperature dependency of output conductance of GaAs FETs," *Microwave J.*, vol. 38, no. 8, pp. 88–94, Aug. 1995.

[3] J. M. Golio, M. G. Miller, G. N. Maracas, and D. A. Johnson, "Frequency-dependent electrical characteristics of GaAs MESFETs," *IEEE Trans. Electron Devices*, vol. 37, pp. 1217–1227, May 1990.

[4] T. Fernandez, Y. Newport, J. M. Zamarillo, A. Mediavilla, and A. Tazon, "High-speed automated pulsed IV measurement system," in *23rd European Microwave Conf.*, Madrid, Spain, Sept. 1993, pp. 494–496.

[5] J. Rodriguez-Tellez, S. Laredo, and R. W. Clarke, "Self-heating in GaAs FETs—A problem?," *Microwave J.*, vol. 37, no. 9, pp. 76–92, Sept. 1994.

[6] J. A. Higgins, "Thermal properties of power HBTs," *IEEE Trans. Electron Devices*, vol. 40, pp. 2171–2177, Dec. 1993.

[7] J. P. Teyssier, P. Bouysse, Z. Ouarch, D. Barataud, T. Peyretaillade, and R. Quere, "40-GHz/150-ns versatile pulsed measurement system for microwave transistor isothermal characterization," *IEEE Trans. Microwave Theory Tech.*, vol. 46, pp. 2043–2052, Dec. 1998.

[8] A. E. Parker and J. B. Scott, "Method for determining correct timing for pulsed *I/V* measurement of GaAs FETs," *Electron. Lett.*, vol. 31, pp. 1697–1698, Sept. 1995.

Numerical Investigation of the Field and Current Behavior Near Lossy Edges

Marco Farina and Tullio Rozzi

***Abstract*—Real circuits involve metallic edges with finite conductivity and nonideal dielectrics. Usually it is more or less implicitly assumed that fields and induced currents behave as if conductors and dielectrics were ideal. In this paper, we show that this assumption is partially erroneous and that the presence of real conductors and dielectrics seems to lead to a simpler and more physical picture, where longitudinal currents are shown to be nonsingular.**

***Index Terms*—Coplanar waveguides, lossy circuits, Maxwell's equations, numerical analysis, wedges.**

I. Introduction

Wedges are sometimes more than a purely academic concern, as recently shown by several authors. In fact, while on the one hand, the knowledge of the field behavior near wedges may be used *a posteriori* in order to check the consistency of numerical solutions, it may be also introduced *a priori* in the numerical solution of integral equations in order to speed up its rate of convergence [1], [2].

Sharp edges are frequently encountered in practice, and, as their sharpness is assumed to be infinite, they may induce singularities in fields and source densities. If, from a theoretical point-of-view, the correct singularity conditions are needed in order to ensure the uniqueness of the field solution [3], in many practical cases, it is just sufficient to have an estimate of the field behavior in order to substantially increase the speed and accuracy of numerical algorithms. This is particularly true when dealing with massively numerical techniques, such as finite differences (FDs) or transmission line methods (TLMs), where the whole space of the analyzed structure has to be cleverly discretized. In these methods, sharp variations in the field would require either great over-meshing or a more expedient inclusion *ab initio* of the known field behavior in the formulation itself. The latter strand is very

Manuscript received February 4, 2000; revised October 10, 2000.
The authors are with the Dipartimento di Eletronnica ed Automatica, Universita degli Studi di Ancona, 60131 Ancona, Italy.
Publisher Item Identifier S 0018-9480(01)05064-5.